Atmosphere Observation by the Method of LED Sun Photometry

A Senior Project

presented to

the Faculty of the Physics Department

California Polytechnic State University, San Luis Obispo

In Partial Fulfillment

of the Requirements of the Degree

Bachelor of Science

by

Gregory Garza

April 2013

Introduction

The focus of this project is centered on the subject of sun photometry. The goal of the experiment was to use a simple self constructed sun photometer to observe how attenuation coefficients change over longer periods of time as well as the determination of the solar extraterrestrial constants for particular wavelengths of light. This was achieved by measuring changes in sun radiance at a particular location for a few hours a day and then use of the Langley extrapolation method on the resulting sun radiance data set.

Sun photometry itself is generally involved in the practice of measuring atmospheric aerosols and water vapor. Roughly a century ago, the Smithsonian Institutes Astrophysical Observatory developed a method of measuring solar radiance using spectrometers; however, these were not usable in a simple hand-held setting. In the 1950's Frederick Volz developed the first hand-held sun photometer, which he improved until coming to the use of silicon photodiodes to produce a photocurrent. These early stages of the development of sun photometry began with the use of silicon photodiodes in conjunction with light filters to measure particular wavelengths of sunlight. However, this method of sun photometry came with cost issues as well as unreliability resulting from degradation and wear on photodiodes.

A more cost effective method was devised by amateur scientist Forrest Mims in 1989 that incorporated the use of light emitting diodes, or LEDs, that are responsive only to the light wavelength that they emit. In a standard circuit involving an LED, current can be run through the LED to produce light of a particular wavelength and energy, specific to the LEDs specifications. Conversely, a current can be *produced* by

introducing light of the same wavelength (as that emitted by the LED) onto the LED. This incident light produces a photocurrent. LED sun photometry exploits this phenomenon to allow for the observation of changes in light intensity at a particular wavelength. This method allows for the determination of how specific wavelengths of sunlight are impacted by changes in the atmosphere in a cost effective manner. It is this LED based sun photometer that provides the premise for this experiment. One other facet of this experiment focuses on observing how the UV index for a given day varies in accordance with the intensity of the sunlight, particularly the shorter wavelengths in the range of UV rays.

The study of sun photometry lends itself to observing changes in air quality. The amount of attenuation in intensity of light and the attenuation coefficient for a particular wavelength of light can be observed to determine the turbidity of the atmosphere, otherwise known as the "degree of haziness." Over extended periods of time, sun photometry can detect changes in the attenuation of sunlight which can be used to discover trends in air quality from issues with air pollution to observing changes resulting from the implementation of aerosol reduction practices. These types of observations regarding changes in the atmosphere over time are an important factor in this experiment as well.

The sun photometer used in this experiment was assembled using a simple operation amplifier circuit to create measureable photocurrents. The total cost of the components necessary to assemble this photometer sum up to roughly $30, making it relatively inexpensive. Some sun photometers are complicated, self regulating systems that automatically adjust themselves to directly face the sun as well as collect data

systematically. This is a much simpler version which is hand-held and is manually pointed at the sun for data measurements.

Data collection was performed numerous times a day to observe the attenuation of the sunlight through the atmosphere and repeated periodically over the span of approximately five months. The result was a series of data sets and plots that show the behavior of the attenuation of sunlight over the course of an extended period of time. Several LEDs were used in this experiment, each operating at a different wavelength, whose attenuation coefficients and solar extraterrestrial constants were measured over the five month time period to observe changes.

Experimental Design

The sun photometer prepared for this project involved the use of a specific set of LEDs to measure the accompanying intensity of the corresponding frequencies of light. To achieve this, the sun photometer was assembled to be an apparatus composed of an op-amp circuit, two 9V batteries to provide a power source (for the op-amp), and a metal fitting to keep an LED light fixed in place. The op-amp component was necessary to make the output readings of photocurrent from the LED photon absorption large enough for observation and measurement. The operational amplifier circuit itself was arranged onto a small circuit board and placed into a small 10×19 centimeter box with one freely removable cover and three apertures drilled into key points.

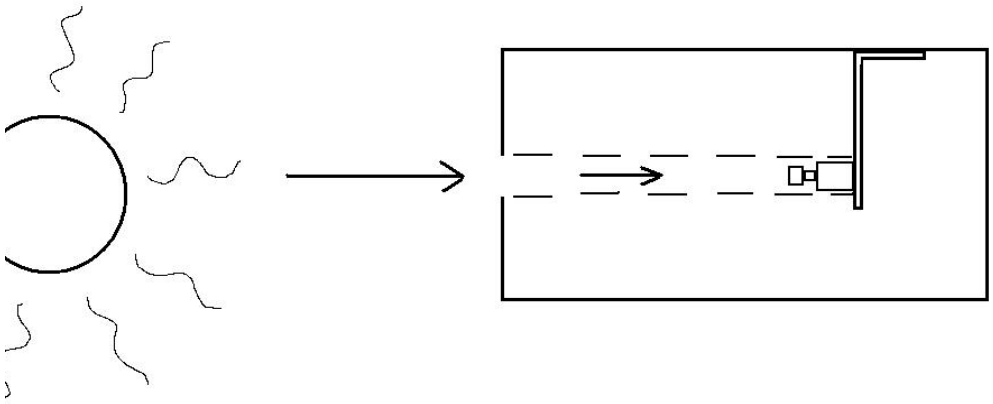

Figure 1: Using the sun photometer to collimate light onto an LED for a sample measurement.

As shown in Figure 1, the primary aperture placed at the left side of the box is used to collimate a beam of light from a distant source onto the LED for an intensity measurement of the LED's response wavelength. The second aperture is drilled into the removable cover of the box in such a way that the hole allows for the LED to be visible from top while minimizing light from other sources. By making the LED visible from the outside, it was simple to determine when the LED was fully illuminated by the light source so that the accuracy of the sunlight intensity measurement was easily verifiable by sight. The third and final aperture is a simple hole, small enough for a wire to be fed through which provides the measured leads for the input and output voltages of the LED on the op-amp. These direct current voltages where read by a Fluke 110 series multimeter for data collection. The fitting for holding the LED in place is held in place through a few bolts placed through some minor drill holes, similarly to two fittings to hold the 9V batteries in place.

Figure 2: The apparatus pictured above attached to the voltmeter with and without the cover on.

The op-amp used for this photometer is the 741 operational amplifier working at a maximum voltage of 9V supplied by two batteries. A diagram of the circuit is shown in Figure 2. The measured voltage used collected as data is the voltage difference between the ground at pin 3 and V_{out} at pin 6.

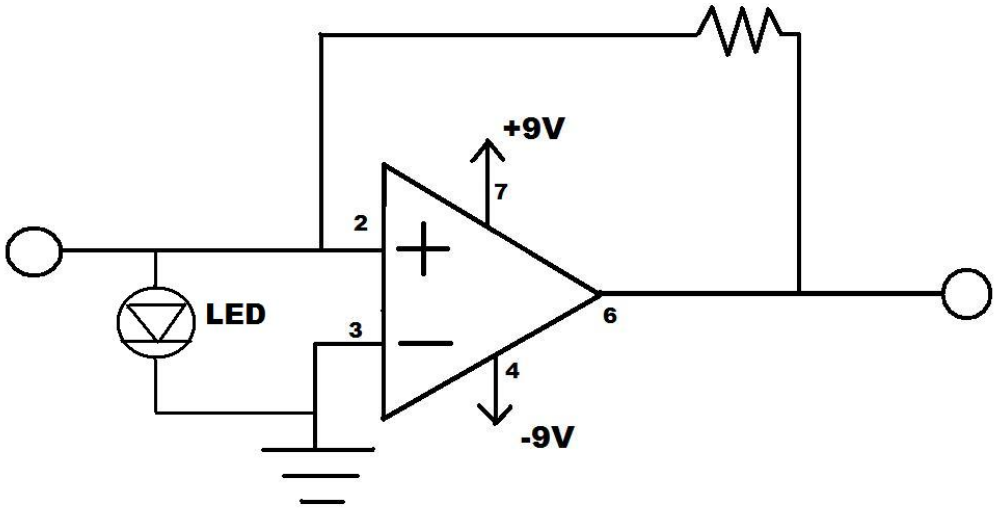

Figure 3: A diagram detailing the op-amp circuit used to deliver readable photocurrents.

The layout of Figure 3 includes the numbered pins at each connection on the 741 op-amp where only the five necessary pins are used. One end of the LEDs is connected to ground while the other serves as the V_{in} for the op-amp. The feedback resistor used here

is one of a reading of 220kΩ allowing for a voltage gain that allows for easily measureable voltage values below the set 9V limit. One final note about the apparatus is the dark current that is present during data collection. A voltage reading of 0.103V is present when the photometer LED is enclosed within a dark space. This voltage bias is subtracted from all data points to give the measured values of voltage caused by sunlight intensity. In this manner, the circuit is a current to voltage converter where the current is driven by the intensity of an LED's response wavelength.

The Physics of Sun Photometry

This project revolved around the measurement of the intensity of the sun's rays at various times during the day in order to observe how the sun rays attenuate in the atmosphere. Of key importance was the sun's altitude at the time that data was taken. Over the course of a day, the sun hit a maximum altitude with respect to the location of data collection. Figure 4 shows a diagram of how the sun's positioning with respect to the sun photometer functions in this experiment.

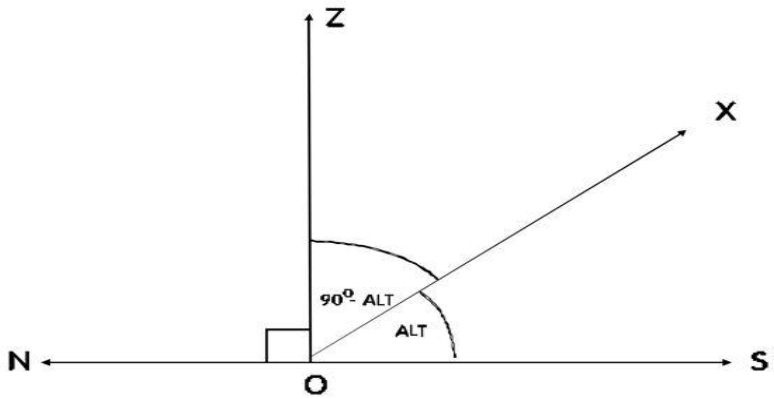

Figure 4: A representation of the sun-altitude positioning where the sun is at a particular altitude with respect to a single position on the surface of the earth.

At midday, the sun is at its maximum altitude where the least atmosphere, and therefore air mass, is in between the photometer and the sun. The sunlight attenuates in

intensity as it travels to the photometer through the atmosphere, which results in a lower photometer reading than the sunlight's maximum reading at the surface of the atmosphere. Of course, the intensity of the sunlight at the surface of the atmosphere cannot be directly measured; however the use of a Langley plot remedies this issue.

As the sun's placement changes in the sky to lower altitudes, the amount of atmosphere in between the data location and sun becomes greater. We expect the attenuation of the sunlight to follow a decay based on a decay curve of the form,

$$I = I_0 e^{-\lambda M} \qquad (1)$$

where I is the intensity of the incident sunlight on the photometer, I_0 is the intensity value at the surface of the atmosphere, M is the mass number, and λ is attenuation coefficient. However, this is a basic form not directly useful for the purposes of the project. By considering that the mass number is a function of altitude and that the intensity of the sunlight is proportional to the voltage reading displayed on the photometer, Equation 1 can be rewritten,

$$V = V_0 e^{-\frac{\lambda}{\sin(\alpha)}} \qquad (2)$$

where α is the altitude of the sun, V is the voltage reading on the photometer, and V_0 is the voltage reading of the photometer at the surface of the atmosphere mentioned before as the solar extraterrestrial constant. Further manipulation of this equation allows for the Langley extrapolation of these quantities.

$$\frac{V}{V_0} = e^{-\frac{\lambda}{\sin(\alpha)}}$$

$$\xrightarrow{yields} \quad ln\frac{V}{V_0} = -\frac{\lambda}{\sin(\alpha)}$$

$$\xrightarrow{yields} \quad lnV = -\frac{\lambda}{\sin(\alpha)} + \ln V_0 \qquad (3)$$

This form of the equation allowed for the indirect measurement of the attenuation coefficient λ as well as the solar extraterrestrial constant given by V_0. By taking voltage data points for the intensity of the sunlight at various times of the day and plotting them against their corresponding sun altitudes, α, a Langley plot was then used to measure λ as the slope of a line and the natural log of V_0 as the y-intercept of the plot. This technique was used to determine the quantities V_0 for each LED frequency as well as observe how the attenuation coefficients for the different frequencies of light would change over the course of the project.

Monochrometer Calibration

One important aspect to the project was the calibration of the photometer, or rather what wavelengths of light the LEDs used in the experiment where actually responding to. In order to discover which wavelengths of sunlight the LEDs responded to, the use of a monochrometer and a continuous white light source was employed to supply an input for the photometer. A bright, continuous 120 watt, light bulb was mounted along an optical rail, placed before a converging lens whose focus was placed onto the input of the monochrometer. The monochrometer was then used to pick out specified wavelengths and feed them into the photometer's various LEDs to determine

what light wavelengths each LED responded to. The experimental setup for this process is shown in Figure 5.

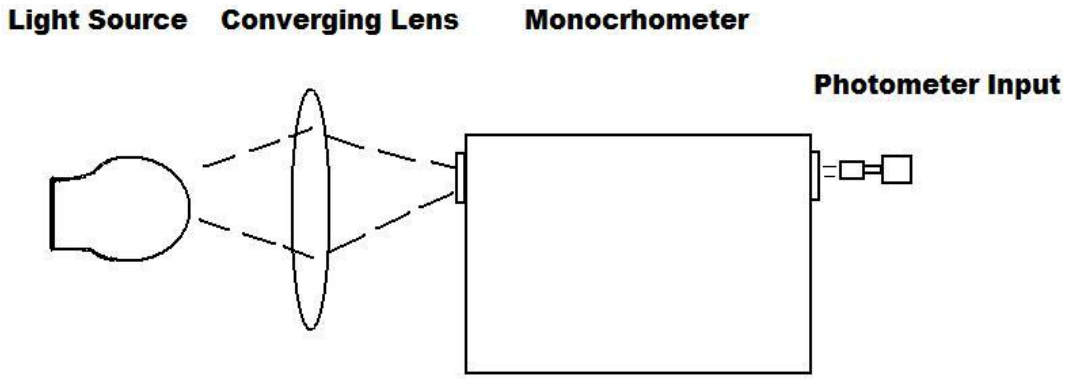

Figure 5: The experimental setup for the wavelength calibration of the sun photometer's six LEDs.

Each LED was tested for responses through the full spectrum of visible light for the 120W bulb; however both the ultraviolet and blue LEDs would not respond to the frequencies present in the white light source. The experiment was repeated for the shorter wavelength LEDs through the use of a mercury lamp which supplied the necessary, shorter wavelength light. Figure 6 shows the response curves for the each six LEDs.

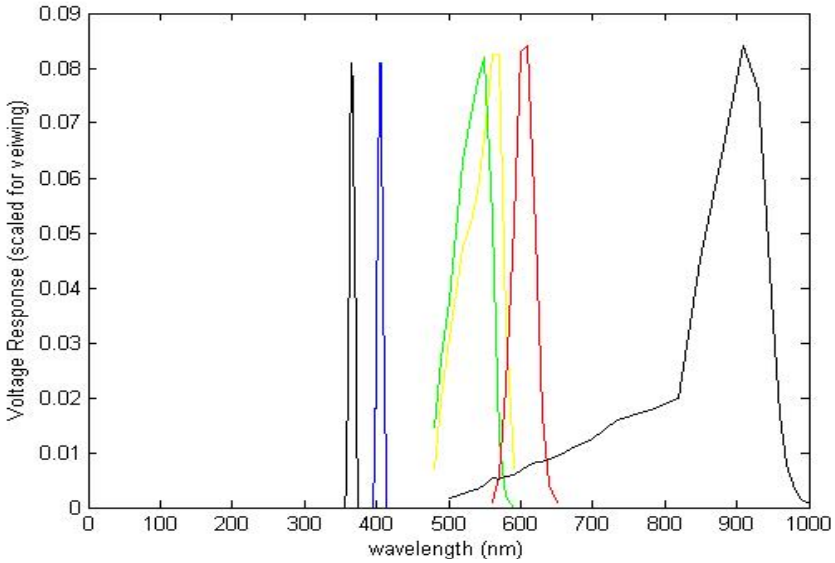

Figure 6: Voltage vs. wavelength. The response wavelengths for the six LEDs. Left to right: UV, blue, green, yellow, red, IR.

It should be noted that the response curves in Figure 6 have their heights scaled to easily show which wavelength each LED had responded to, and that there was a large amount of variation in the maximum intensities of the response curves. The method used to produce these curves involved shifting the light source passed by the monochrometer by small wavelength steps on the scale of one to ten nanometers per data point depending on how drastically the voltage fluctuated between steps. Each LED responded around a particular wavelength with the exception of the infrared LED which can be seen in Figure 6 to have a larger range of infrared wavelengths that it weakly responded to, including that of some visible light. Based on Figure 6, the LEDs then have response wavelengths with measured values given in Table 1.

LED Type	UV	IR	Yellow	Red	Blue	Green
Response Wavelength (nm)	366 ± 5	910 ± 50	565 ± 30	605 ± 20	405 ± 4	550 ± 50

Table 1: The response wavelengths for each of the six LEDs with a margin of error based upon the full width half maximum.

Calculations and Graphs

As described, by using the data taken for the attenuation of sunlight, Langley plots were generated for each data set for various days. Each data set yielded an attenuation coefficient and a value for the solar extraterrestrial constant, V_0, for each day that they corresponded to.

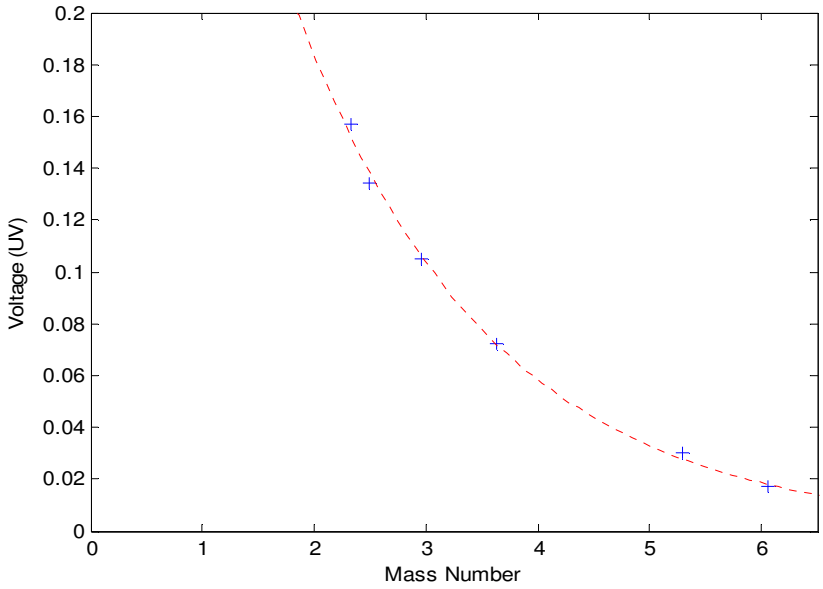

Figure 7: Voltage vs. mass number. UV voltage data points for 11/20/12, fitted with a decay curve.

The attenuation curve pictured by Figure 7 is an example for the type of curve that each data set taken over a day ideally yields. The mass number varies with the inverse of the sine of the altitude and the expectation was that the light rays attenuate according to the altitude. By taking this decay curve and rearranging it into a Langley plot, the attenuation coefficient as well as the value for V_0 were then obtainable. By using the same set of UV data for 11/20/12, the accompanying Langley plot is pictured below in Figure 8.

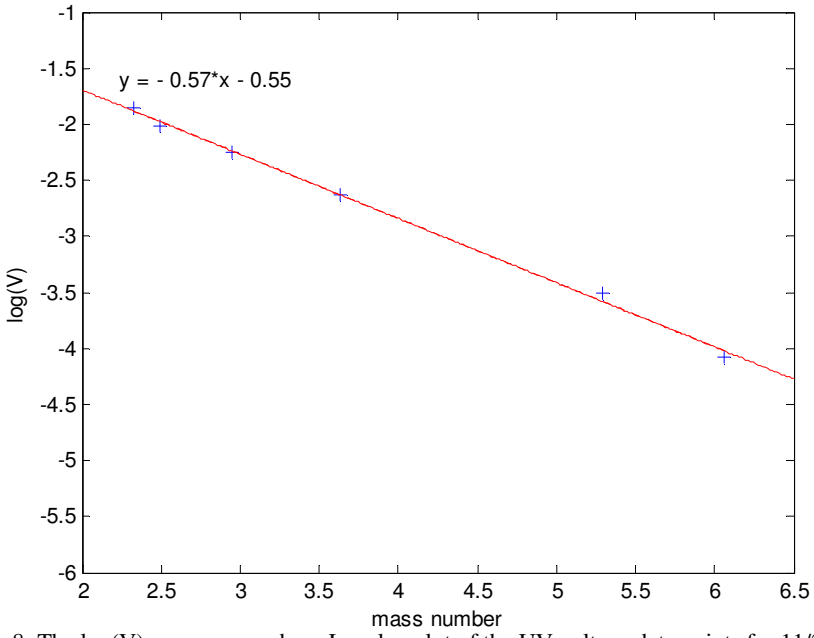

Figure 8: The log(V) vs. mass number. Langley plot of the UV voltage data points for 11/20/12, fitted with a linear function.

By using the fit shown in Figure 8, we are able to determine the coefficient of attenuation as $\lambda = -.57$ and the voltage reading at the top of the atmosphere for UV rays as the value $V_0 = .578$ V by using the fact that $V_0 = \exp(-.55)$.

However, the plots shown in Figures 7 and 8 are only examples for one data set for one day. With such a large number of data points, this process was repeated for 48 different days for each LED over the course of several months starting on October 9, 2012 and ending on February 26, 2013. The individual data points compose a massive data set and are shown over the course of the last few months in Figures 9 through 14. The following analysis only considers the overall attenuation of the intensity as shown by these figures.

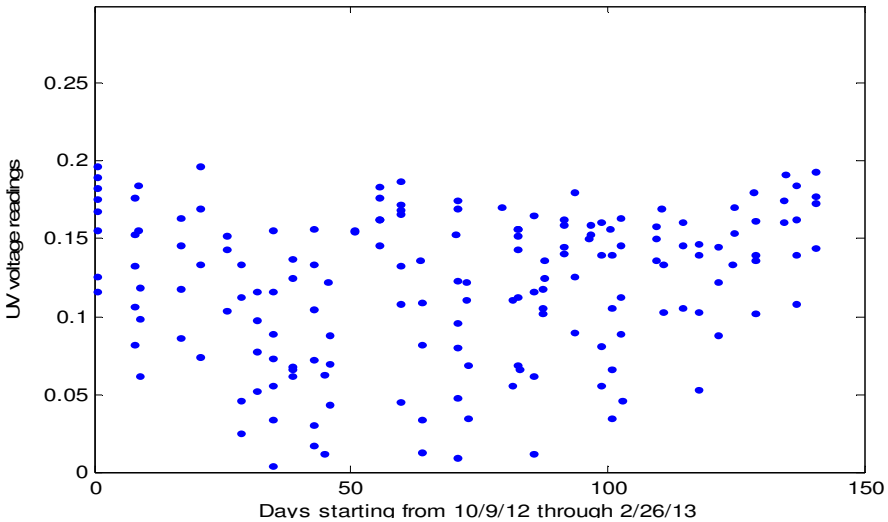

Figure 9: Voltage vs. days. The voltage data set for the UV LED.

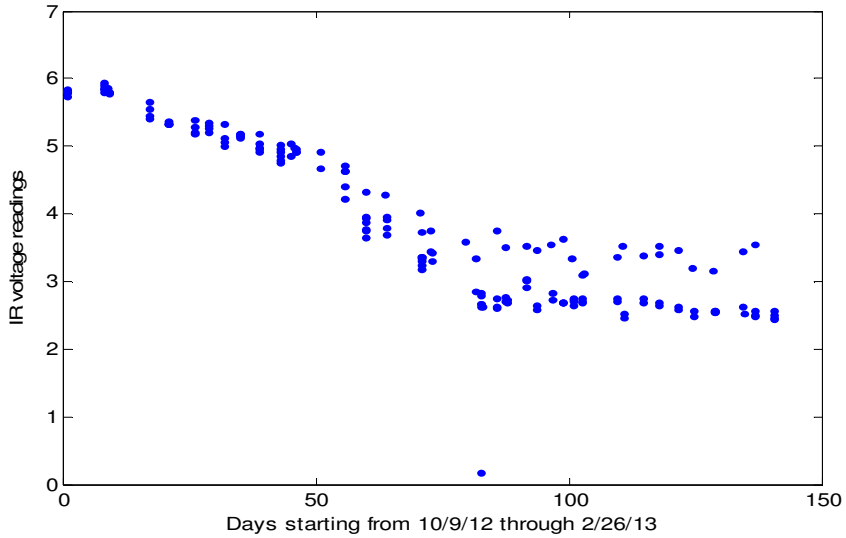

Figure 10: Voltage vs. days. The voltage data set for the IR LED.

From the above plots we can see a number of interesting behaviors over the past month. Each data set has a different intensity, so the scatter of the data points over the voltage appears greater due to lower intensity values. Most of the data points show how the different response wavelengths attenuate and have actually changed over the course of the experiment. Since the largest voltage data points coincide to voltage values taken at the highest altitude times, the change in the amount of attenuation between days became apparent.

The UV data set shows relatively little change over the course of the experiment and shows that the UV rays are not as intense as others. There appear to be a few dips in the maximum voltage that occurs at roughly from day 25 to day 55 and from day 60 to day 125, but the general intensity of UV rays appears to be highly consistent.

The IR plot shows two very interesting behaviors. Firstly, the plot shows a very clear and steady decay in the intensity for IR data points until roughly day 75. Since the IR LED responds to a rather large range of wavelengths as shown in the monochrometer calibration section, some particular range of wavelengths within that response curve could be attenuating more than the others. There is a possibility that there could be a dynamic relationship between what wavelengths are attenuated more strongly. The second thing to note is the outlier point that becomes prominent around day 75. Possibly an issue of LED temperature, this becomes noticeable as for the second half of the plot, there is one point that sticks far above the rest.

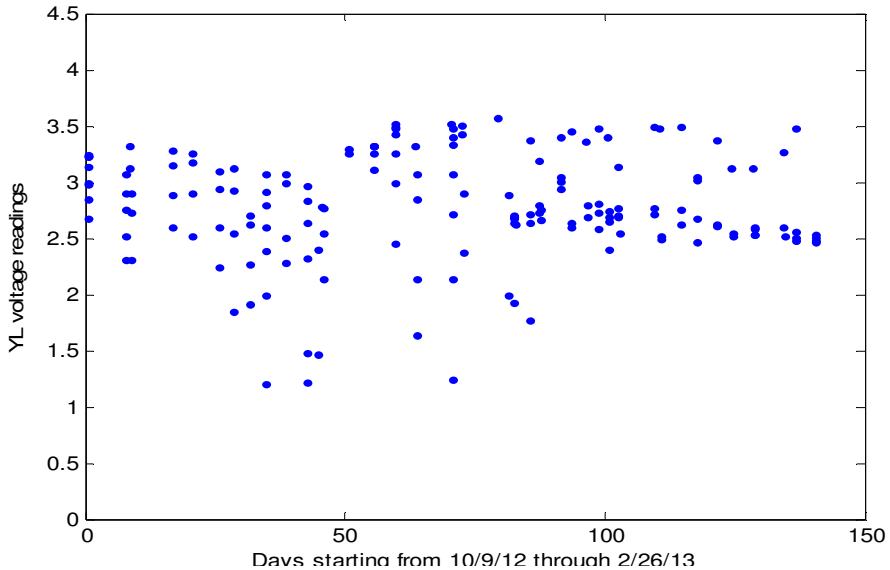

Figure 11: Voltage vs. days. The voltage data set for the yellow LED.

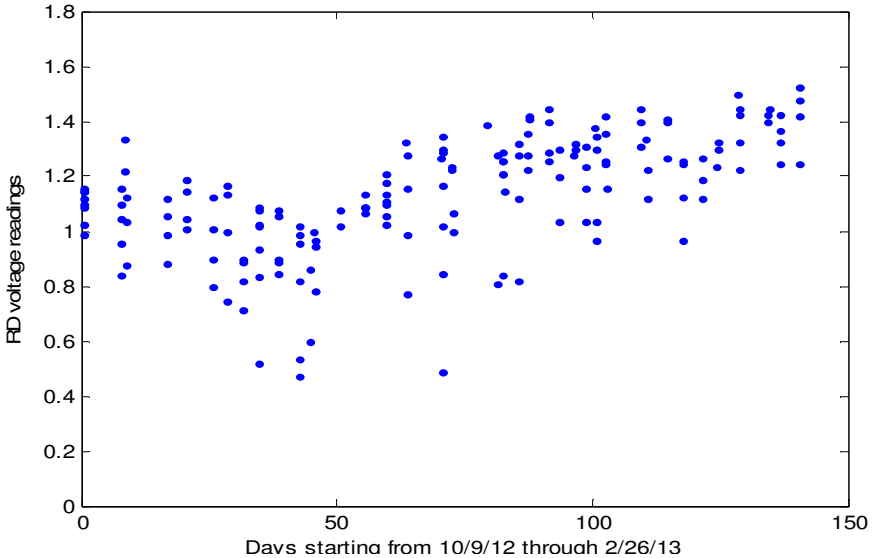

Figure 12: Voltage vs. days. The voltage data set for the red LED

The next two plots are those of the yellow and red LEDs. The yellow LED shows steady behavior although, once again, the outlier problem becomes apparent. Not considering the outlier in this case it appears that there was actually a decrease in attenuation over the day 50 to 75 period. Aside from the IR LED, none of the other LEDs suffered from this outlier problem. Red shows a slow increase in intensity attenuation from the beginning of the experiment to roughly day 50, after which the attenuation decreases until roughly day 75. The amount that the red intensity attenuates is then steady until the end of the experiment.

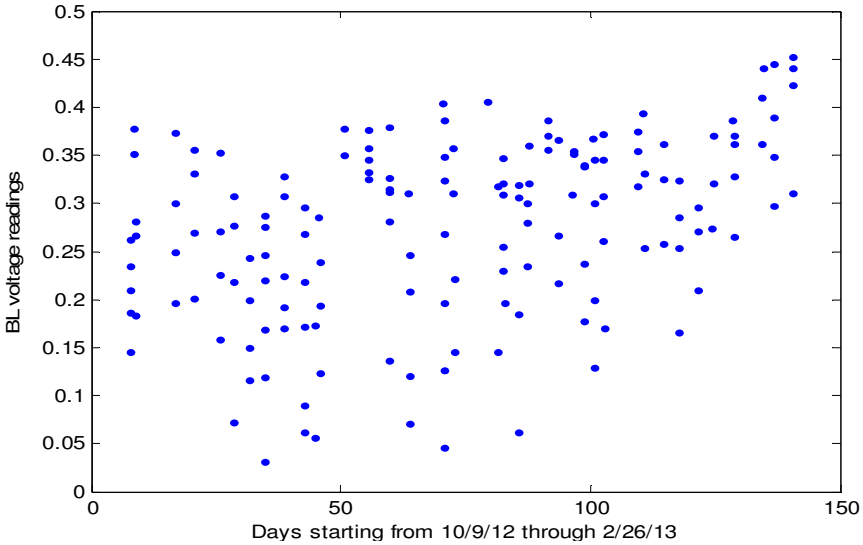

Figure 13: Voltage vs. days. The voltage data set for the blue LED.

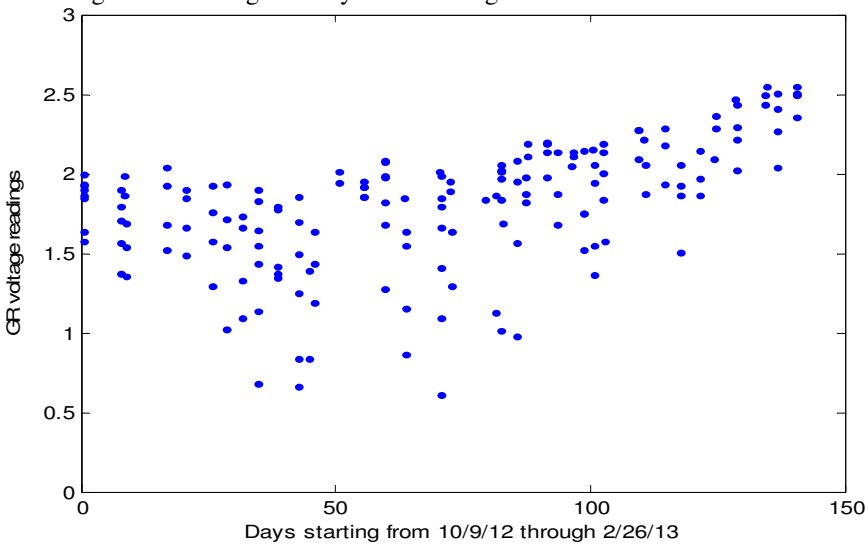

Figure 14: Voltage vs. days. The voltage data set for the green LED.

The blue LED plot shows a steady rise and decrease pattern over the course of the experiment. Similarly to the UV LED, the response wavelength for the blue LED is not particularly strong compared to the others. The green LED shows a very clear and steady increase all the way until the end of the experiment. With these sets of data, the values for the V_0 and λ are then obtainable.

Calculation of V_0 and λ

The values for V_0 and λ were then calculated for each day by using the decay curves from these data sets and performing a Langley extrapolation. Each data set yielded a measurement for the solar extraterrestrial constant V_0. The average value of the calculated constant for each day was then measured along with the standard deviation for the measurements. This method of averaging the values of V_0 yields the approximated results given in Table 2.

	UV	IR	Yellow	Red	Blue	Green
V_0	0.549 ± 0.03	5.12 ± 0.25	4.66 ± 0.27	1.56 ± 0.05	0.824 ± 0.041	3.10 ± 0.19

Table 2: The average extraterrestrial attenuation coefficients with standard deviations.

Using the same method, of course, yielded the attenuation coefficients for the data sets as well. Each day yielded a unique attenuation coefficient, and in a similar manner, we were able to see how the sunlight attenuates with respect to the amount of atmosphere and the time of day. On the same time scale, from October 9, 2012 and ending on February 26, 2013, the attenuation coefficients were plotted with error bars in Figures 15 through 20.

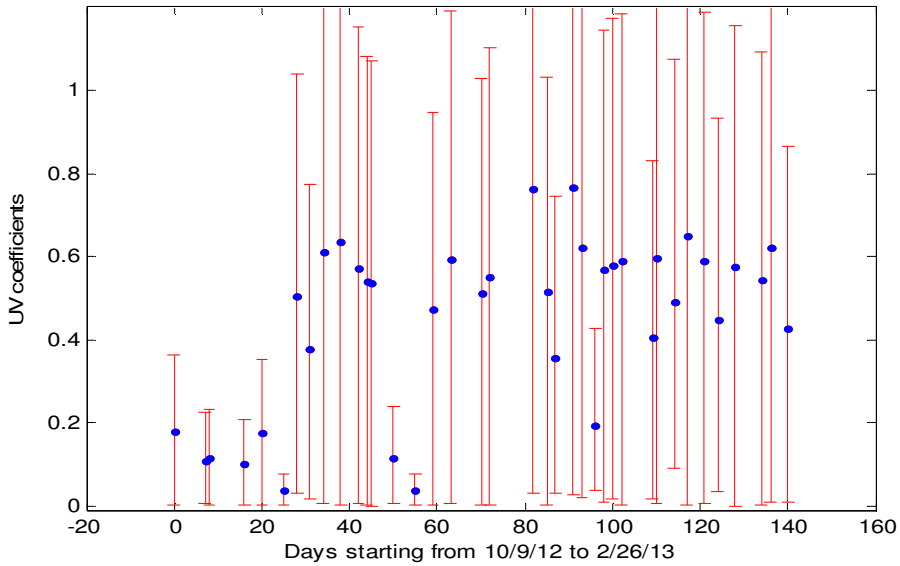

Figure 15: Attenuation coefficient vs. days. This plot shows how the UV LED varied over an extended period of time.

Figure 15 shows the attenuation coefficients for the UV LED; however, some explanation is needed to describe some of the behavior that the plot displays. Early data points show that the attenuation coefficients are generally lower and appear to have a smaller margin of error, which is a trend that persists for the following plots as well. There appears to be a change in the atmosphere according to the data from 11/3/12 as there were no changes in the method of data taking to warrant this. This change in coefficients possibly reflects the change in the weather during the winter season. Something that should also be noted is the data points that occur at days 50 and 55. These points show wildly varying margins of error and very large deviation from the norm for most of the plots shown here. Days 50 and 55 were data points taken under the most cloudy and most poor weather conditions of the entire experiment and serve as an example of what unsteady weather can do to the data sets. Overall, however, UV data sets show a general attenuation coefficient of typically 0.6 for sunlight of the wavelength $\lambda = 366\text{nm}$.

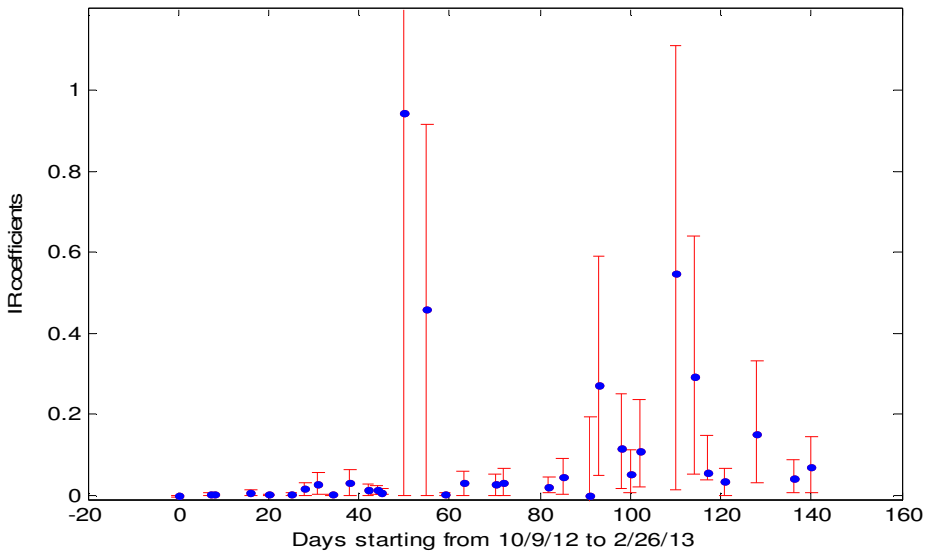

Figure 16: Attenuation coefficient vs. days. This plot shows how the IR LED varied over an extended period of time.

As stated for Figure 10, it is important to note how the outlier points for the IR data sets change the attenuation coefficients in Figure 16, particularly later on. For the earlier, more reliable points, the IR attenuation coefficients are typically in the range of 0.03 for sunlight roughly of the wavelength $\lambda = 910$nm. That is, it appears that visible light does not attenuate as strongly as lower wavelengths, but the factor of the very large range of response wavelengths for the IR LED is likely also a culprit for this phenomenon as well.

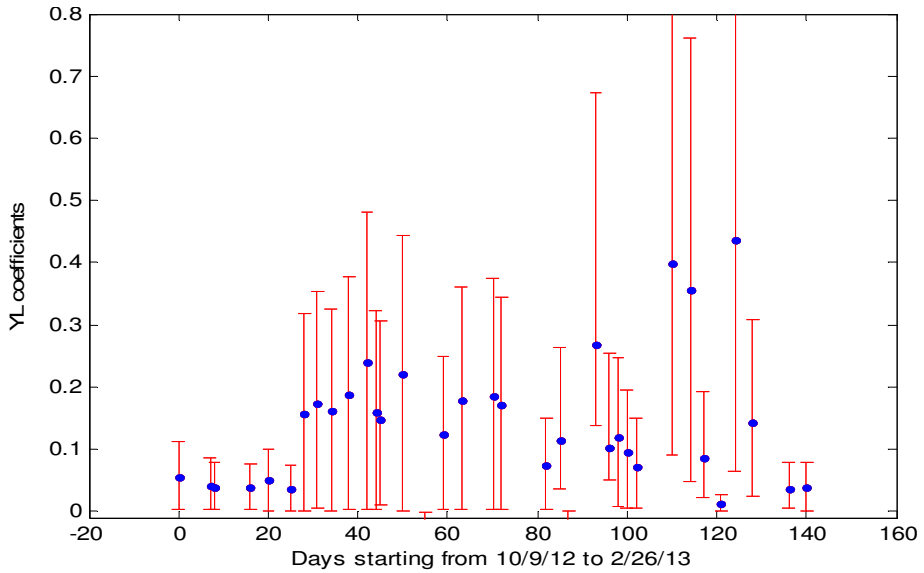

Figure 17: Attenuation coefficient vs. days. This plot shows how the yellow LED varied over an extended period of time.

Similarly to the IR LED, the yellow LED suffered from the same outlier problem which results in the larger margin of error on the later attenuation coefficients. By choosing to consider the best data sets in this case as well, the yellow LED tended to yield values of attenuation coefficients typically on the scale of 0.18 for sunlight with a wavelength $\lambda = 565\text{nm}$.

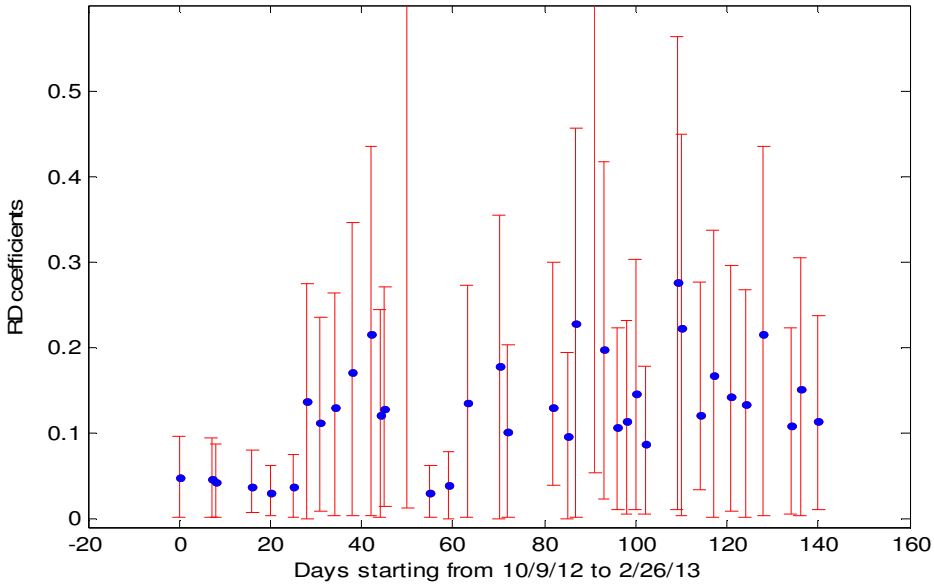

Figure 18: Attenuation coefficient vs. days. This plot shows how the red LED varied over an extended period of time.

The red LED, along with blue and green, yielded one of the more consistent data sets as can be seen in Figure 18. For red, the attenuation coefficients were generally centered on 0.13 for sunlight wavelengths around $\lambda = 605$nm.

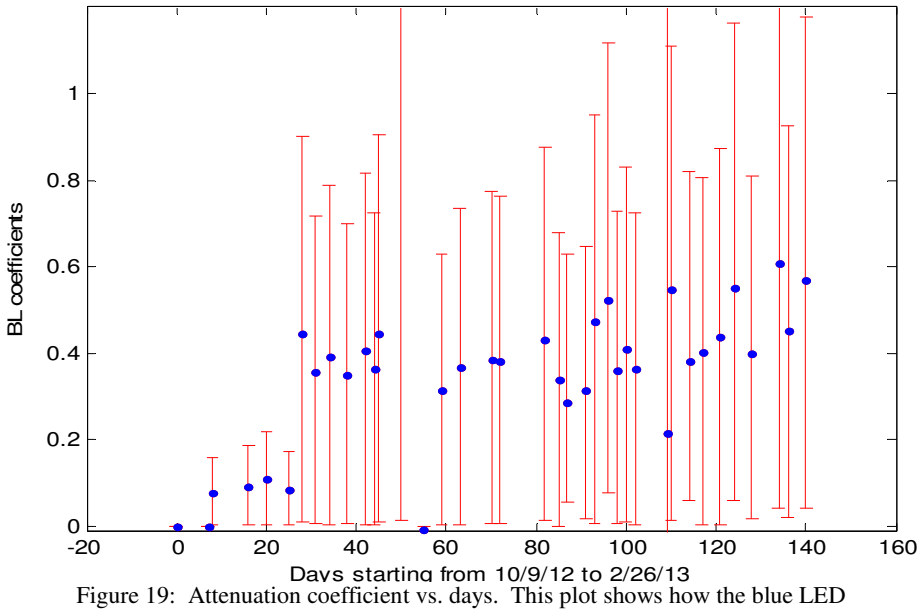

Figure 19: Attenuation coefficient vs. days. This plot shows how the blue LED varied over an extended period of time.

The blue LED, similarly, shows very consistent behavior for the attenuation coefficients. Light of wavelength $\lambda = 405$nm appears to have attenuation coefficients in the atmosphere centered largely on 0.4.

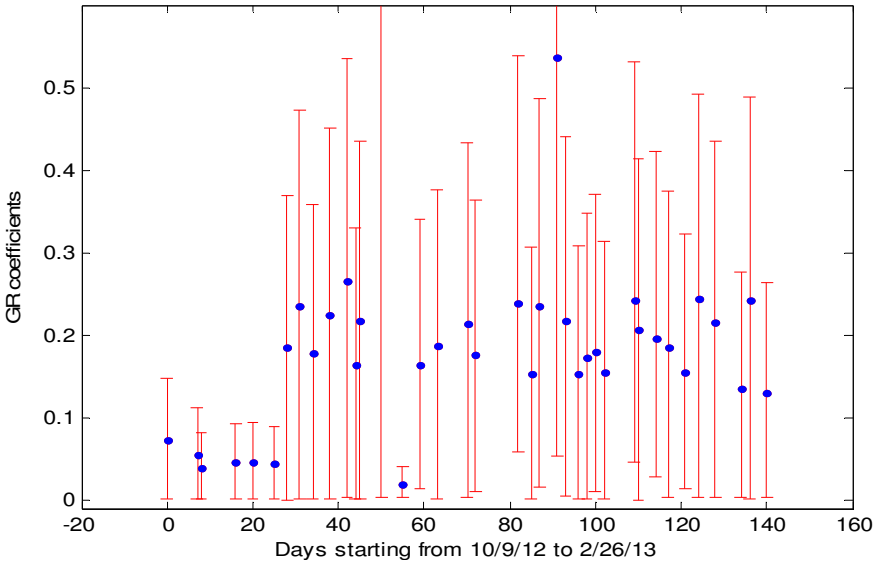

Figure 20: Attenuation coefficient vs. days. This plot shows how the green LED varied over an extended period of time.

Lastly, the green LED also yields consistent attenuation coefficients. For sunlight with a wavelength of $\lambda = 550$, the attenuation coefficients generally center on 0.2.

The UV index and ray attenuation

This section focuses on how the UV index varies in accordance with sunlight attenuation. The UV index serves the purpose of a warning in the form of a scale that ranges from 0 to 11+ that informs a person as to the intensity of UV rays for a particular day in a particular location. The rating of 0 serves to show that there is miniscule UV radiation and a rating of 11 or higher implies dangerously high levels of radiation. The goal for this section was to observe how measured intensity for both the UV and blue LED's fluctuate over the sun's passing in comparison to the UV index itself.

For this experiment, data for the UV and blue LEDs were taken from 10am to 3pm on March 15, 2013 on the hour as well as using data taken from the United States Environmental Protection Agency on the UV index for that day. The reason that data is

only taken on the hour is due to the fact that the UV index is given hourly by the EPA system. Figure 21 shows how the intensity of the λ_{bl} = 405nm and λ_{uv} = 366nm light rays varied with the UV index.

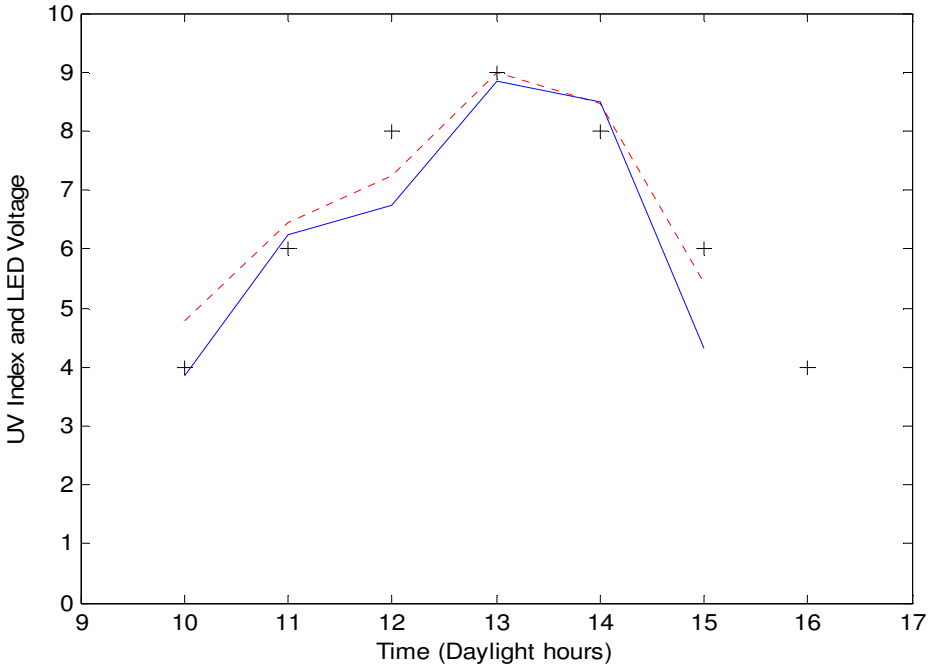

Figure 21: UV index and LED voltage vs. time. This plot shows how UV intensity varies well with the actual UV index. The plus points represent the UV index, while the dashed line is for the UV LED and the solid line is for the blue LED readings. LED voltages are scaled for comparison.

The intensity of UV radiation clearly mirrors the UV index very well. From this, it would be expected that the sunlight intensity and the UV index share a linear relationship. However, since the UV index is listed in terms of a scale, the data needed to be multiplied by multiplication factors of $28V^{-1}$ for the UV voltages and $16V^{-1}$ for the blue voltages. These multiplication factors are, of course, unique to the LEDs used in this experiment, and would not necessarily reflect all UV and blue LEDs. For another plot comparison, Figure 22 and Figure 23 show how the voltages vary based on corresponding UV index readings.

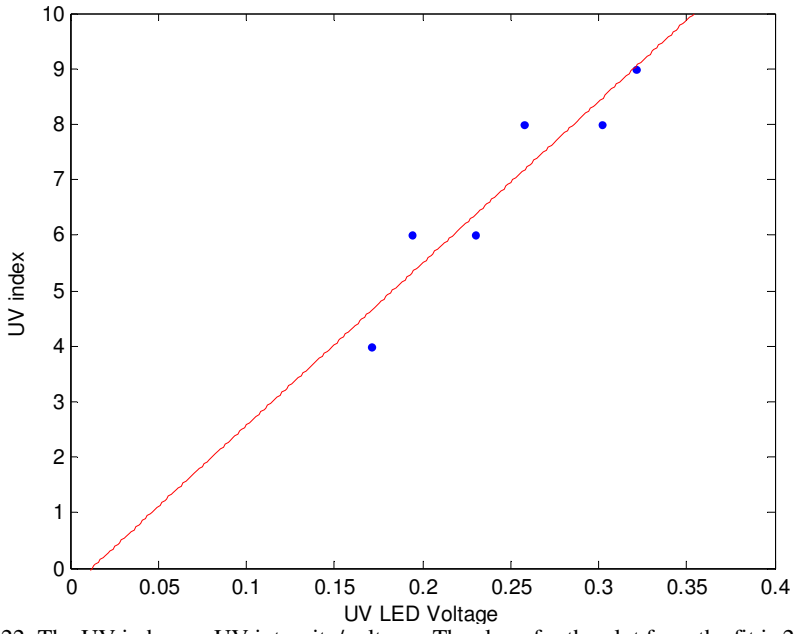

Figure 22: The UV index vs. UV intensity/voltage. The slope for the plot from the fit is $29.2V^{-1}$.

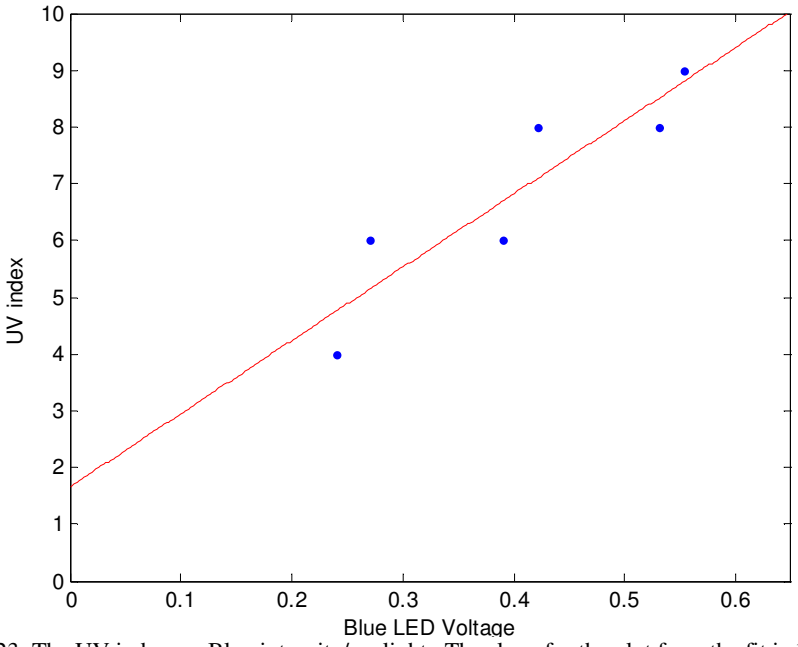

Figure 23: The UV index vs. Blue intensity/sunlight. The slope for the plot from the fit is $12.9V^{-1}$.

Both of these plots show a roughly linear relationship between the intensities and the UV index. The small amount of scatter present is very likely due to changes in turbidity of the atmosphere over the span of a day. In particular, notice how the intensity plot in Figure 21 has points fluctuate from being higher and lower than the behavior of the UV index. This effect produces the scatter present in Figures 22 and 23.

Conclusion

By having taken periodic data, the long term behavior of the sunlight as well as attenuation of sunlight became much clearer. Figures 9-14 helped to determine the overall behavior of the intensity of the various light wavelengths. Particularly the wavelengths corresponding to the IR LED as well as the green LED show very clear increases and decreases steadily over time. As far as attenuation coefficients are concerned in Figures 15-20, it appears that the UV and blue LEDs show the largest attenuation coefficients in comparison to all other LEDs, particularly compared to IR. This appears to indicate that the atmosphere attenuates shorter wavelengths more strongly than longer ones. Lastly, the UV index correspondence to the intensity of sunlight shows a definite direct relationship. Figures 21-23 show clear a relationship between observed UV and blue LED sunlight intensity and the UV index such that they are essentially linear. A fix that could be made to minimize the margin of error present in some of the plots could be in the using of LEDs with smaller response wavelength curves like in Figure 6. Also, choosing a more clear weather time of year to take data such as spring and summer rather than fall and winter would eliminate some of the outlier points that exist and allow for more frequent data taking than was sometimes possible.